Journal of Power Sources 267 (2014) 700–705

Contents lists available at ScienceDirect

Journal of Power Sources

journal homepage: www.elsevier.com/locate/jpowsour

Strontium titanate: An all-in-one rechargeable energy storage material

Juliane Hanzig [a, *, 1], Matthias Zschornak [a, b, 1], Melanie Nentwich [a], Florian Hanzig [a], Sibylle Gemming [b], Tilmann Leisegang [c], Dirk C. Meyer [a]

[a] Institut für Experimentelle Physik, TU Bergakademie Freiberg, Leipziger Straße 23, 09596 Freiberg, Germany
[b] Institut für Ionenstrahlphysik und Materialforschung, Helmholtz-Zentrum Dresden-Rossendorf, Bautzner Landstraße 400, 01314 Dresden, Germany
[c] Fraunhofer-Technologiezentrum Halbleitermaterialien, Am St.-Niclas-Schacht 13, 09599 Freiberg, Germany

HIGHLIGHTS

- We present a proof of concept of a new scalable all solid state energy storage.
- $SrTiO_3$ serves as anode, cathode as well as electrolyte.
- We present a defect based charge and discharge mechanism.
- Thermodynamic deduction of the exergonic reaction by density functional theory.

ARTICLE INFO

Article history:
Received 14 December 2013
Received in revised form
19 March 2014
Accepted 5 May 2014
Available online 2 June 2014

Keywords:
Solid state energy storage
Transition metal oxides
Defects
Density functional theory

ABSTRACT

Redistribution of oxygen vacancies in a strontium titanate single crystal is caused by an external electric field. We present electrical measurements during and directly after electroformation, showing that intrinsic defect separation establishes a non-equilibrium state in the transition metal oxide accompanied by an electromotive force. A comprehensive thermodynamic deduction in terms of theoretical energy and entropy calculations indicate an exergonic electrochemical reaction after the electric field is switched off. Based on that driving force the experimental and theoretical proof of concept of an all-in-one rechargeable $SrTiO_3$ single crystal energy storage is reported here.

1. Introduction

Research on electrochemical energy storage is closely related to materials with ionic or even covalent bonded systems as, *e.g.*, transition metal oxides, for battery components. Working as host structures for intercalation of Li ions in lithium ion batteries [1], they also have great potential as catalysts in metal–air batteries [2] as well as electrode material in supercapacitors [3] and are applied as solid electrolytes in sodium–sulfur batteries [4] or solid oxide fuel cells [5]. Based on their high abundance, low cost, environmental compatibility and chemical stability as well as manifold electrical and chemical properties, transition metal oxides are particularly suitable for new concepts of redox-based energy storage. One opportunity of generating new concepts is the synergy of data and energy storage technologies.

Hence, perovskite-type transition metal oxides are known to have great potential as storage material in resistive random-access memory (RRAM) devices [6]. Typical non-volatile memory cells are realized in metal-insulator-metal (MIM) stacks. Currently, there exist different pictures of switching mechanisms in the literature [7]. In general, they are based on changes in resistivity, defining a high resistance and a low resistance state which differ several orders of magnitude, which is also observed in dependency of oxygen partial pressure at high temperatures [8,9]. Application of high electric fields leads to local structural [10] and compositional [7,11] changes in dielectric materials. In this process, oxygen vacancies $V_O^{\bullet\bullet}$ act as most mobile defects in oxides, revealing a mobility of $2 \cdot 10^{-10}$ cm^2 Vs^{-1} at room temperature [10]. Therefore, a redistribution of oxygen vacancies as well as an establishment of an oxygen concentration gradient takes place, where defects are responsible

* Corresponding author.
E-mail address: juliane.hanzig@physik.tu-freiberg.de (J. Hanzig).
[1] These authors contributed equally to this work.

http://dx.doi.org/10.1016/j.jpowsour.2014.05.095
0378-7753/

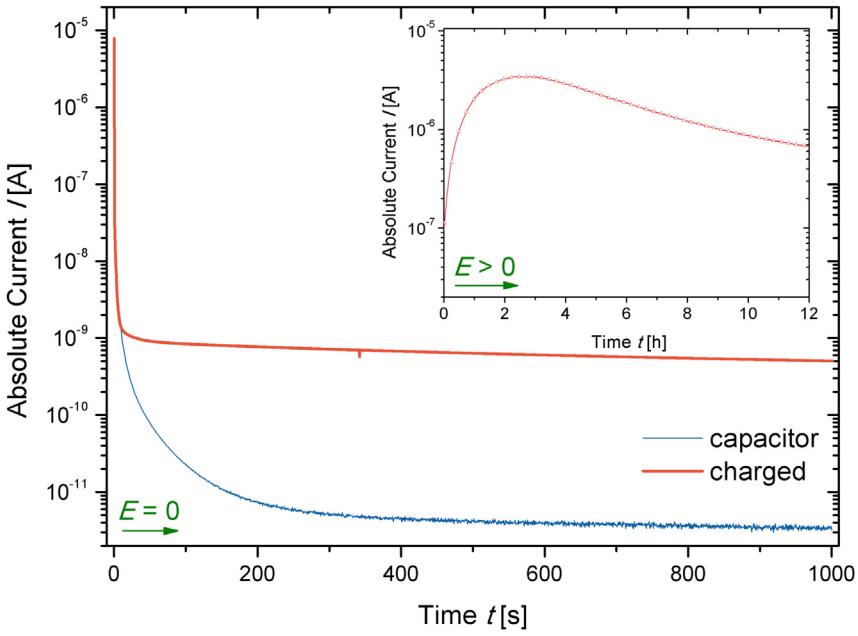

Fig. 1. Charging and discharging behavior of a $SrTiO_3$ single crystal energy storage. The inset shows the time-dependent current $I(t)$ during electroformation (charging process). The discharging current of the charged $SrTiO_3$ cell after electroformation shows a significant increase in comparison to a capacitor with $SrTiO_3$ dielectric charged at 100 V for a few seconds.

for localized reduction and oxidation of transition metal ions [12], respectively. Accumulation of oxygen vacancies is further known to form defect clusters [13,14] to gain energy. The accompanied disproportionation of redox couples in the applied electrical field stores energy electrochemically which causes an electromotive force, as already reported by Waser et al. [15] in MIM stacks. This is a requirement for galvanic cells and determines the characteristic cell voltage.

Strontium titanate is a model material, crystallizing in cubic structure with space group $Pm\bar{3}m$, which hosts a manifold of excellent physical properties based on its crystallographic and electronic structure. Various applications can be found in the literature, *e.g.*: gem-stone (fabulite) [16], high-*k* dielectric [17], oxygen sensor [18], superconductor [19], photo-catalytic material [20], resistive random access memory [6,21]. Here, we report on the experimental investigation and theoretical description of charging and discharging processes of $SrTiO_3$ single crystals to demonstrate the potential of perovskites for scalable electrochemical energy storage.

2. Materials and methods

The presented electrochemical cell is composed of an etched [22] as-grown $SrTiO_3$ single crystal coated on both sides with titanium electrodes [10], which is needed for applying the external electric field homogeneously. Some crystals have been prepared with structured front side electrodes, revealing different contact sizes. Single crystals investigated here were of $5 \times 5 \times 0.1$ mm^3 or $10 \times 10 \times 0.1$ mm^3 dimension in (001) orientation ordered from CrysTec GmbH (Berlin). All samples showed the same qualitative behavior, quantitative results depend on the crystal real structure. Electroformation of the strontium titanate single crystals was performed using electric fields in the order of 10^6 V m^{-1} where the electric current flow through the crystal was recorded. Electrical measurements were performed in complete absence of light. Time-dependent current measurements have been conducted with a Keithley 4200 SCS.

3. Results

In a Gibbs–Helmholtz picture it is obvious that in thermodynamic equilibrium real structures at finite temperature are determined by defects, caused by the energy gain due to entropy increase. Having the lowest formation energy [23], oxygen vacancies play the key role in ionic transport in transition metal oxides. Assuming a homogeneous distribution of $V_O^{\bullet\bullet}$ throughout the entire crystal in the initial state ($E = 0$), they are redistributed, based on their charge, during electroformation ($E > 0$) [7,24,25], which is illustrated in the inset of Fig. 1. Consequently, oxygen vacancies accumulate at the cathode (negative pole) and deplete at the anode (positive pole), which is accompanied by structural changes at the oxygen-rich side, as reported previously [10]. Such a forced defect separation leads to an establishment of a non-equilibrium state in the crystal and involves the titanium to be reduced and oxidized [12], respectively. If the external electric field is switched off, a reversed current can be measured (see Fig. 1) due to the redistribution of the $V_O^{\bullet\bullet}$. Hence, locally there exist different driving forces [15] to equilibrate the $SrTiO_3$ single crystal again: (a) the Nernst potential V_N having a redox couple with exergonic character, (b) the diffusion potential V_d regarding the concentration gradient of mobile oxygen vacancies, (c) the Gibbs–Thomson potential V_{GT} in terms of an enhanced surface energy of dendrites and additionally, (d) a strain potential V_s caused by the elastic distortion of a reversible phase present at the anode after electroformation [10]. Fig. 1 shows the discharging behavior of a formed $SrTiO_3$ cell in comparison with a capacitor structure using strontium titanate as dielectric. A significantly higher current is observed after voltage shut down if the cell is additionally charged by electroformation.

A drift-driven redistribution of $V_O^{\bullet\bullet}$ establishes a concentration gradient accompanied by a change in oxidation state of titanium and can be considered as charging process. Therefore, a Nernst potential originates from the local minimization of the free enthalpy over the chemical potential gradients of the active species at both half-cells, which in sum act voluntarily. In our setup the active species are Ti atoms with oxidation states Ti^{2+} in the vicinity

of two adjacent oxygen vacancies (vacancy cluster) [14,13], Ti^{3+} next to one oxygen vacancy (diluted vacancies) and Ti^{4+} in stoichiometric strontium titanate unit cells (see Fig. 2). At room temperature the crystal inherently acts as a separator as well, blocking all ionic movement but the diluted vacancy. Upon charging the applied external electric potential forces the change of Ti valence states at the electrodes, here, using Kröger–Vink notation [26]:

$$\text{Anode}: \quad Ti'_{Ti} \rightarrow Ti^{\times}_{Ti} + e' \tag{1}$$

$$\text{Cathode}: \quad Ti'_{Ti} + e' \rightarrow Ti''_{Ti} \tag{2}$$

The limiting process for the reactions and according current is the migration of diluted vacancies through the crystal to the vacancy rich region to form clusters [13,14]. Due to its increased electronic conductivity it acts as virtual electrode [7]. Next to the changes of Ti oxidation states a gradient of the chemical potential of oxygen vacancies is developed. Upon discharging the Nernst potential drives the inverse redox reactions at the electrodes. An overall redox reaction can be written as comproportionation:

$$\text{Crystal}: \quad Ti^{\times}_{Ti} + Ti''_{Ti} \rightarrow 2\,Ti'_{Ti} \tag{3}$$

The Gibbs free energy difference ΔG between discharged and charged state is defined by the Gibbs–Helmholtz equation in relation to the enthalpy H, the temperature T and the entropy S of the system,

$$\Delta G = (H_{2Ti^{3+}} - H_{Ti^{2+/4+}}) - T\cdot(S_{2Ti^{3+}} - S_{Ti^{2+/4+}}). \tag{4}$$

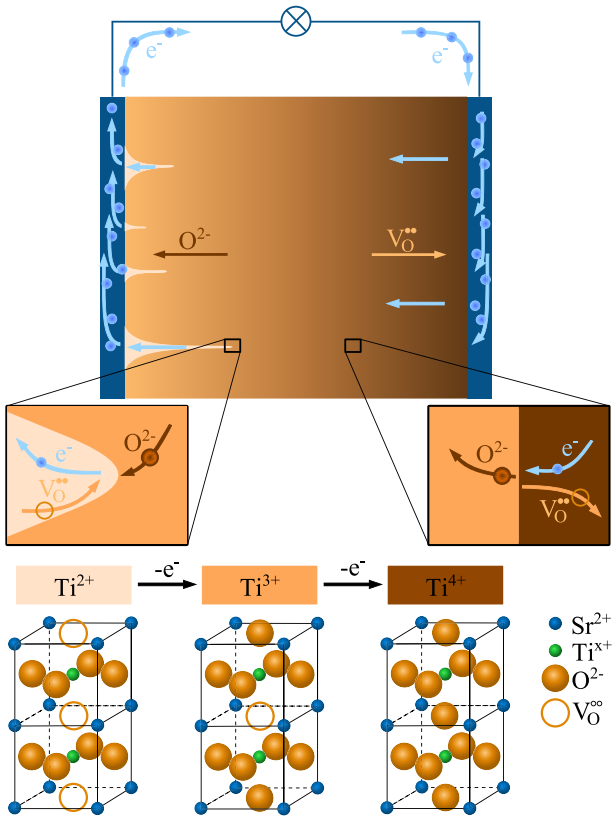

Fig. 2. Discharging process of a $SrTiO_3$ single crystal energy storage. The non-equilibrium state of accumulated vacancies at the negative electrode region of the crystal arranged in dendrites causes the electromotive force and the related redox process. Vacancy clusters (Ti^{2+}) dissolve into stoichiometric $SrTiO_3$ (Ti^{4+}) and form diluted oxygen vacancies (Ti^{3+}) which homogenously fill the entire crystal at equilibrium.

The change in enthalpy H of the Ti^{3+} equilibrium diluted vacancy state in respect to the Ti^{2+}/Ti^{4+} charged state with vacancy chains along neighboring octahedra on one side and the stoichiometric Ti^{4+} state on the other was estimated according to the structures shown in Fig. 2. The total energy of the supercell with one oxygen vacancy (Ti^{3+}) was hereby compared to the total energy of the supercell representing the vacancy chain (Ti^{2+}/Ti^{4+}) by means of density functional theory (DFT) calculations using the ABINIT pseudopotential code [27] with LDA Teter extended norm-conserving potentials. A kinetic energy cutoff of 823 eV and an $8\times8\times8$ Monkhorst-Pack k-point grid for the stoichiometric $SrTiO_3$ cell was applied and convergence with respect to supercell size ensured. All internal coordinates have been relaxed to forces less than 2 meV $Å^{-1}$ and the cell parameters of the supercells have been set to the relaxed parameters of the stoichiometric $SrTiO_3$ cell. The clustered vacancy state is favored with $\Delta H = 0.13$ eV per vacancy or $\Delta H = 1.3\cdot10^{15}$ eV for the dimensions of the bigger crystal volumes mentioned above, assuming a maximum vacancy density of $1\cdot10^{18}$ cm^{-3} [10]. The entropy of mixing [28] was calculated making two assumptions: first, an equal distribution of the vacancies on all oxygen sites $N_1 = 5.0\cdot10^{20}$ in the discharged state (crystal size divided by the volume of the unit cell with lattice parameter [29] $a = 3.901$ Å) and second, a number of $n = 1\cdot10^{16}$ vacancies for the $SrTiO_3$ crystal. The case of the discharged state can be calculated as an n-combination of N_1 elements without repetition and the charged state as an n-combination of N_2 elements with repetition, where $N_2 = 5.32\cdot10^{14}$ is the number of oxygen sites at the interface of the vacancy cluster region (crystal size of the contact area divided by the square of lattice parameter a). Using the Boltzmann formula, the binomial coefficient, and the Stirling formula the entropy of mixing yields

$$\Delta S = 1.00\cdot10^{13}\ \text{eV K}^{-1}. \tag{5}$$

That means for the enthalpy at room temperature

$$\Delta G < 0, \tag{6}$$

so discharging is an exergonic reaction as required.

Additionally, on a local basis, the concentration gradient of the mobile oxygen vacancies within the bulk drives the redox reaction upon discharging. The corresponding voltage can be estimated from Valov's et al. [15] equation 5. As dendrites are formed [15], it is to be expected that the strain in the interface region costs additional energy while charging the cell. This energy can be estimated from Gibbs–Thomson equation 6 mentioned there as well [15] and will additionally drive the cell during discharging. Potentially there is a fourth energy contribution from forming a distorted phase at the anode region, next to the dendrites at the cathode, during the charging process. This phase could be identified as migration-induced field-stabilized polar phase [10] and its degeneration will contribute while the crystal relaxes to the equilibrium state of $SrTiO_3$.

Now, it is demonstrated how $SrTiO_3$ serves as all-in-one rechargeable energy storage. Fig. 3a, depicts different I–V sweeps, realizing a hold time of 1 h during each cycle. Initially, increasing the external voltage (I) leads to a linear current increase (note logarithmic scale). During step (II), which is interpreted as the beginning of electroformation, a sufficient forming voltage is passed to move oxygen vacancies through the single crystal. In spite of voltage decrease a higher current can be seen, where (III) represents the maximum of the forming current (see inset of Fig. 1) and a maximum number of mobile defects in motion. More and more redistributed $V_O^{\bullet\bullet}$ arrive at the cathode (charging process), which is superimposed by the voltage decrease of the external voltage,

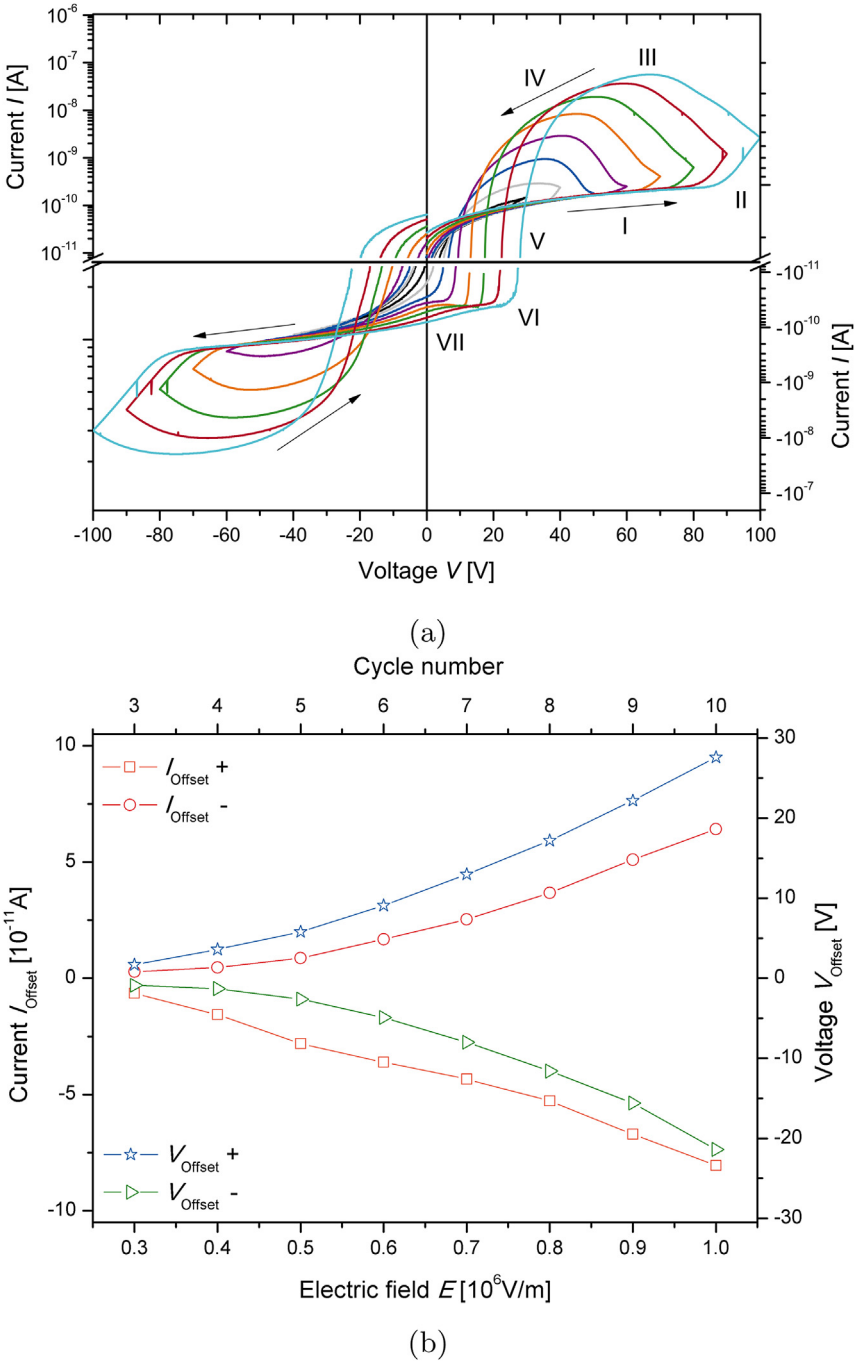

Fig. 3. Rechargeability of a $SrTiO_3$ electrochemical cell shown for different voltage sweeps. (a) Exemplar *I–V* characteristics of an as-grown $SrTiO_3$ single crystal coated with titanium demonstrating the charging (I–V) and discharging (VI–VII) processes. (b) Offset currents and offset voltages depend on the applied electric field.

followed by a current drop (IV). At $I = 0$ A the electrochemical cell is arranged in an electrochemical equilibrium (V), where the external voltage is sufficient to hold the charged state. A further voltage decrease leads to an opposite current (VI), which means that the applied voltage is incapable to keep the oxygen vacancies at the cathode. Hence, this serves as proof for the battery behavior. Now, the charged $SrTiO_3$ cell acts against the external voltage and as internal voltage source (discharging process). At $U = 0$ V (VII) a non-zero current can still be measured, evidencing the electromotive force of the system. Continuing the cycle to negative voltages a similar current voltage behavior can be discussed accordingly. Thus, a specific characteristic can be found in the functionality of the electrochemical cell, where anode and cathode are simply determined by the polarity of the charging process.

In the following certain aspects concerning $SrTiO_3$ as all-in-one rechargeable energy storage material are discussed in more detail. The voltage-dependent electrochemical cell-equilibrium is summarized in Fig. 3b, showing the offset voltages V_{Offset} and currents I_{Offset} for the different voltage sweeps. The increase of up to quadratic order depicts an additive formation behavior within the crystal, which can be attributed to the afore mentioned components of the electromotive force. Hereby, the Nernst potential is assumed to be constant, whereas the diffusion potential V_d and the strain potential V_s increase due to enhanced lattice deformation

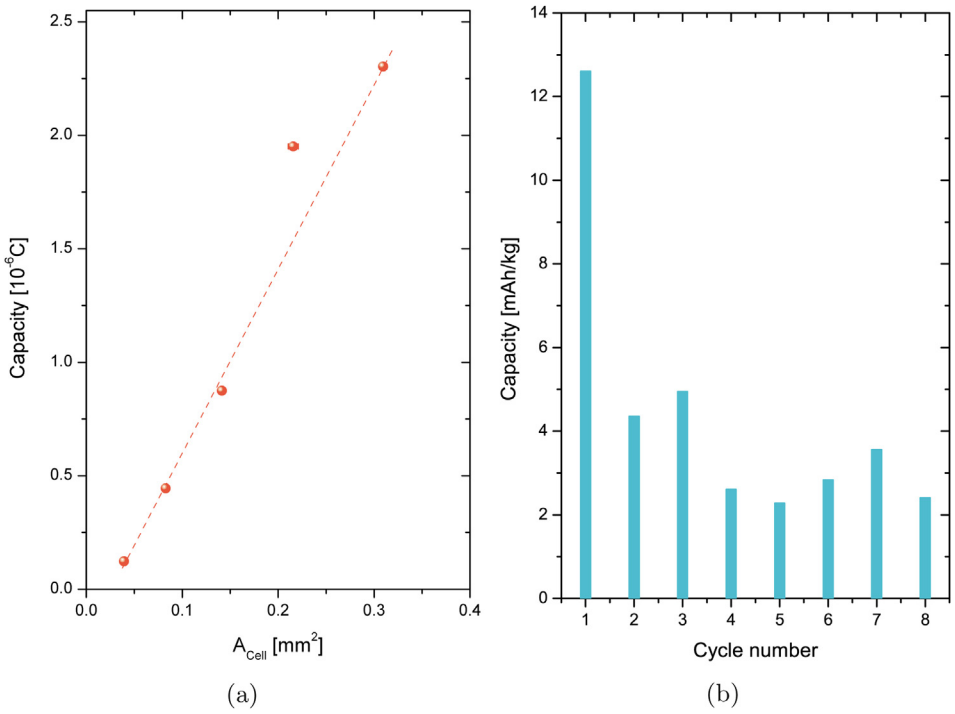

Fig. 4. (a) Capacity of the electrochemical cell depends linearly on the contact area A_{Cell}, which suggests that the defects in a given crystal volume directly contribute to the cell performance. (b) After a first electroformation cycle, the capacity of the electrochemical cell remains comparatively constant during several cycles, which shows the stability of the oxide with periodic charging and discharging.

[10] revealing linear and quadratic dependence respectively, as well as a more pronounced oxygen vacancy concentration gradient at higher voltages and a higher state of ordering (entropy of mixing).

Capacity considerations obviously show a dependence on the contact area of the current collector (see Fig. 4a), scaling linearly. The corresponding cell volume which is charged during electroformation thus correlates directly with the number of redistributed mobile defects [10] and therefore allows a linear up-scaling of capacity. To study the stability of the electrochemical cell in respect to rechargeability, consecutive measurements on another single crystal have been performed. In accordance it is possible to show the rechargeability of the cell (see Fig. 4b), whereby the capacity varies within ±1.5 mAh kg^{-1} during 8 cycles.

4. Discussion

Successfully, a new concept for rechargeable electrochemical energy storage based on defect separation by an external electric field in materials with high dielectric constants, like strontium titanate, was presented. As a major advantage the transition metal oxide serves as anode and cathode as well as electrolyte and separator in one material for energy storage applications. The usage of an environmentally friendly and low cost material is another benefit in the development of renewable energy. Similarly, $SrTiO_3$ features thermal as well as mechanical and chemical stability associated to minor wastage and cycle stability. The presented cells could be cycled several times at capacities of 3 mAh/ kg^{-1}. It is obvious that the standard details of the presented energy device have to be optimized, regarding other established electrochemical energy storage, *e.g.* lithium ion batteries, metal air batteries or redox flow batteries. But this proof of concept initiates further investigation and transfer of the results to thin films. In particular, higher capacities could be achieved in accordance to an increase of the defect density or the up-scaling of the cell volume, which is directly related. A sufficient voltage improves keeping the charged state at full capacity. As defined by this proof of concept, the all-in-one rechargeable energy storage is especially suitable for electrochemical short-term storage, like supercapacitors. To enhance the Nernst potential, it is suggested to employ transition metal oxides with redox couples, revealing a higher difference of their redox potentials, such as Mn, Cr or Fe. Likewise, combinations of oxides may be envisaged to establish a bifunctional redox couple to increase the cell voltage. For such processes to occur, defect diffusion across interfaces has to be realized.

Acknowledgment

This work has been performed within the joint research project "CryPhysConcept – Mit Kristallphysik zum Zukunftskonzept elektrochemischer Energiespeicher" (03EK3029A) which is financially supported by the Federal Ministry of Education and Research (BMBF). The authors would like to thank the CryPhysConcept team for valuable discussions, especially F. Meutzner for graphical assistance. Part of this work has been performed within the HGF-funded Virtual Institute MEMRIOX ("Memory Effects in Resistive Ion-beam Modified Oxides", VH-VI-422). M. Nentwich thanks for financial support within the European Social Fund (Europa fördert Sachsen) and Ministry of Science and Art of Saxony via Landesinnovationsstipendium (100111044).

References

[1] A. Kraytsberg, Y. Ein-Eli, Adv. Energy Mater. 2 (8) (2012) 922–939.
[2] F. Cheng, J. Chen, Chem. Soc. Rev. 41 (6) (2012) 2172–2192.
[3] Y. Zhang, H. Feng, X. Wu, L. Wang, A. Zhang, T. Xia, H. Dong, X. Li, L. Zhang, Int. J. Hydrogen Energy 34 (11) (2009) 4889–4899.
[4] X. Lu, G. Xia, J.P. Lemmon, Z. Yang, J. Power Sources 195 (9) (2010) 2431–2442.
[5] M.C. Tucker, J. Power Sources 195 (15) (2010) 4570–4582.
[6] A. Sawa, Mater. Today 11 (6) (2008) 28–36.
[7] R. Waser, R. Dittmann, G. Staikov, K. Szot, Adv. Mater. 21 (25–26) (2009) 2632–2663.

[8] N. Chan, R. Sharma, D. Smyth, J. Electrochem. Soc. 128 (8) (1981) 1762.
[9] K. Szot, W. Speier, R. Carius, U. Zastrow, W. Beyer, Phys. Rev. Lett. 88 (7) (2002) 75508.
[10] J. Hanzig, M. Zschornak, F. Hanzig, E. Mehner, H. Stöcker, B. Abendroth, C. Röder, A. Talkenberger, G. Schreiber, D. Rafaja, S. Gemming, D.C. Meyer, Phys. Rev. B 88 (2) (2013) 024104.
[11] T. Baiatu, R. Waser, K. Härdtl, J. Am. Ceram. Soc. 73 (6) (1990) 1663–1673.
[12] T. Leisegang, H. Stöcker, A. Levin, T. Weißbach, M. Zschornak, E. Gutmann, K. Rickers, S. Gemming, D. Meyer, Phys. Rev. Lett. 102 (8) (2009) 87601.
[13] D.D. Cuong, B. Lee, K.M. Choi, H.S. Ahn, S. Han, J. Lee, Phys. Rev. Lett. 98 (11) (2007) 115503.
[14] N. Shanthi, D.D. Sarma, Phys. Rev. B 57 (4) (1998) 2153.
[15] I. Valov, E. Linn, S. Tappertzhofen, S. Schmelzer, J. van den Hurk, F. Lentz, R. Waser, Nat. Commun 2014.
[16] Y.I. Vorob'yev, A.A. Konev, Y.V. Malyshonok, G.F. Afonina, A.N. Sapozhnikov, Int. Geol. Rev. 26 (4) (1984) 462–465.
[17] J. Robertson, J. Vac. Sci. Technol. B Microelectron. Nanometer Struct. 18 (2000) 1785.
[18] W. Menesklou, H.J. Schreiner, K.H. Härdtl, E. Ivers-Tiffée, Sens. Actuators B Chem. 59 (2–3) (1999) 184–189.
[19] J.F. Schooley, W.R. Hosler, M.L. Cohen, Phys. Rev. Lett. 12 (1964) 474–475, http://dx.doi.org/10.1103/PhysRevLett.12.474.
[20] M.G. Walter, E.L. Warren, J.R. McKone, S.W. Boettcher, Q. Mi, E.A. Santori, N.S. Lewis, Chem. Rev. 110 (11) (2010) 6446–6473.
[21] K. Szot, W. Speier, G. Bihlmayer, R. Waser, Nat. Mater. 5 (4) (2006) 312–320.
[22] G. Koster, B.L. Kropman, G.J.H.M. Rijnders, D.H.A. Blank, H. Rogalla, Appl. Phys. Lett. 73 (20) (1998) 2920–2922.
[23] M.J. Akhtar, Z. Akhtar, R.A. Jackson, C. Catlow, A. Richard, J. Am. Ceram. Soc. 78 (2) (2005) 421–428.
[24] J. Blanc, D.L. Staebler, Phys. Rev. B 4 (1971) 3548–3557.
[25] S.K. Mohapatra, S. Wagner, J. Appl. Phys. 50 (1979) 5001–5006.
[26] F.A. Kröger, H.J. Vink, in: F. Seitz, D. Turnbull (Eds.), Solid State Physics, vol. 3, Elsevier, 1956, pp. 307–435.
[27] X. Gonze, J. Beuken, R. Caracas, F. Detraux, M. Fuchs, G. Rignanese, L. Sindic, M. Verstraete, G. Zerah, F. Jollet, M. Torrent, A. Roy, M. Mikami, P. Ghosez, J.-Y. Raty, D. Allan, Comput. Mater. Sci. 25 (3) (2002) 478–492.
[28] H. Föll, http://www.tf.uni-kiel.de/matwis/amat/def_en/, 2013.
[29] Y.A. Abramov, V. Tsirelson, V. Zavodnik, S. Ivanov, I. Brown, Acta Crystallogr. B Struct. Sci. 51 (6) (1995) 942–951.